Published in "Superconductor Science and Technology 22(12): 125014, 2009"
which should be cited to refer to this work.

The effect of citric and oxalic acid doping on the superconducting properties of MgB_2

N Ojha[1], V K Malik[2], Rashmi Singla[1], C Bernhard[2] and G D Varma[1]

[1] Department of Physics, Indian Institute of Technology Roorkee, Roorkee-247667, India
[2] Department of Physics and Fribourg Centre for Nanomaterials-FriMat, University of Fribourg, Chemin du Musee, CH-1700 Fribourg, Switzerland

E-mail: gdvarfph@iitr.ernet.in

Abstract

In this paper we report the effect of carbon doping on the structural and superconducting properties of MgB_2 using citric and oxalic acids as carbon sources. The bulk polycrystalline samples have been synthesized via a standard solid state reaction route with composition $MgB_2 + x$ wt% of citric and oxalic acids ($x = 0$, 5 and 10). The x-ray diffraction results reveal the formation of dominantly MgB_2 with only a small amount of impurity phase MgO and substitution of C at the B site of MgB_2 for both dopants. Improvements in the upper critical field (H_{C2}), irreversibility field (H_{irr}) and high field (>2.5 T) critical current density (J_C) have been observed on C doping in the samples. The correlations between superconducting properties and structural characteristics of the samples are described and discussed in this paper.

1. Introduction

Since its discovery in 2001 [1], a great deal of work has been done to improve the superconducting properties, such as the critical current (J_C), the upper critical field (H_{C2}) and the irreversibility field (H_{irr}), of MgB_2. The introduction of additional flux pinning centers and connectivity enhancement of the grains are both necessary to increase the irreversibility field (H_{irr}) and the critical current density (J_C) to the levels required for commercial applications. As the critical current density is affected by the upper critical field, improvement in its H_{C2} is essential for practical applications of MgB_2. H_{C2} can be improved by the introduction of disorder through various processes such as chemical doping [2–6], irradiation [7] and various thermochemical processing techniques [8–10]. Further, MgB_2 has two superconducting gaps, which allow tuning of the upper critical fields (H_{C2}) by controlling different defect sublattices relative to the orthogonal hybrid bands. Nanosized precursor particles have been used extensively to improve H_{C2} of MgB_2 [10–13], but it is a great challenge to achieve homogeneous distribution of a small amount of nanodopants within the matrix materials through solid state mixing. There are always agglomerates of nanoadditives in the precursor because it is very difficult to disperse nanoparticles [14]. Among the large number of dopants used, the C-containing compounds, such as SiC, carbon nanotubes, B_4C etc [15–17], are the most promising additives for the enhancement of J_C, H_{irr} and H_{C2}. However, it has been found that for various sources of C doping, the reaction leading to the substitution of C for boron (B) cannot be achieved at the same temperatures as the MgB_2 formation reaction due to their poor reactivity. Recently, many workers have suggested using carbohydrates as the C-source for substitution of C at the B site of MgB_2 [14, 18–22]. Carbohydrates provide active elemental carbon above their decomposition temperature, resulting in C substitution for B, which introduces more disorder in the lattice. In the present investigation we have used two carbohydrates, citric and oxalic acids, as dopants to introduce C into the MgB_2 lattice. We have studied the structural and superconducting properties of the doped samples.

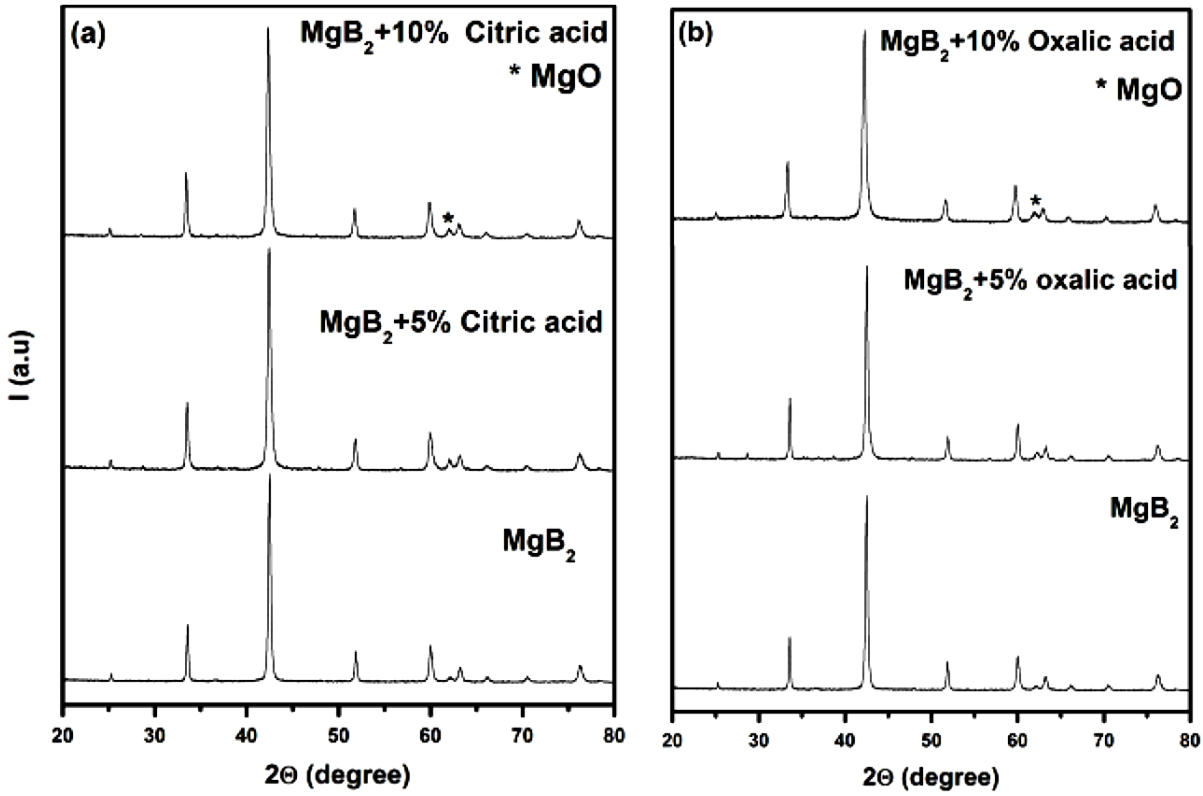

Figure 1. XRD patterns of citric acid doped (a) and oxalic acid doped (b) MgB_2.

2. Experimental details

The bulk polycrystalline samples of MgB_2 were synthesized by an *in situ* reaction process with the addition of citric acid and oxalic acid. Appropriate amounts of Mg and B to form MgB_2 were mixed with x wt% ($x = 0$, 5 and 10) of citric or oxalic acid in an agate mortar. The mixture was thoroughly ground and the resulting powder was pressed to form rectangular pellets. The pellets were sintered at 850 °C in an argon (Ar) atmosphere for 3 hours. The phase identification of the samples was carried out using x-ray diffractometry with Cu Kα radiation. The microstructure of the samples was studied using a field emission scanning electron microscope (FESEM). The resistivity measurements in different magnetic fields (0–8 T) were carried out using a physical properties measurement system (PPMS) (Quantum Design-6000). The irreversibility field (H_{irr}), and $H_{C2}(T)$ were deduced using the criteria 10% and 90% of normal state resistivity. The DC magnetic measurements were carried out with a vibrating sample magnetometer in the PPMS.

3. Results and discussion

The x-ray diffraction (XRD) patterns of citric acid and oxalic acid doped MgB_2 samples are shown in figure 1. The XRD patterns clearly reveal the presence of the hexagonal crystal structure of MgB_2 with a small amount of MgO impurity for both dopants. From the XRD results we do not find traces of any other secondary phases in the samples. The peak intensity of MgO increases with increasing doping concentration of both dopants. To study qualitatively the variation of MgO phase in the samples we have estimated the volume fraction of MgO in the samples from the peak intensities of the XRD patterns using the relation: volume fraction of MgO phase $= \Sigma$ integrated peak intensities of MgO phase/Σ integrated intensities of all phases. From this we find that the volume fraction of MgO in the sample increases with doping concentration of citric and oxalic acid. This is possibly because of the presence of oxygen atoms in the dopant. The lattice parameters determined from the XRD data are given in table 1. It can be seen that the lattice parameter a decreases with increasing wt% of citric and oxalic acids in the samples (see figure 2(a)). This confirms the substitution of C at the B site of MgB_2. Thus, the carbon atoms produced from the decomposition of the carbohydrates are incorporated into the MgB_2 lattice. The actual C substitution level for doped samples has been estimated from the value of the lattice parameter a calculated from the XRD data using the relation $a = 3.0861–0.438\,09x$, where x is the composition of carbon corresponding to the formula $Mg(B_{1-x}C_x)_2$ [23]. The estimated values of x are given in table 1. It can be seen that the actual carbon substitution level of the citric acid doped samples is slightly higher than that of the corresponding oxalic acid doped one. This is possibly due to more carbon atoms in the molecular formula of citric acid ($C_6H_8O_7$) as compared to that of oxalic acid ($C_2H_6O_5$). The full width at half maximum (FWHM) of the 101 peak shows an increasing trend as the carbohydrate addition level increases (see figure 2(b)). This indicates that crystallinity of the samples decreases with increasing carbon content. We have also estimated the strain

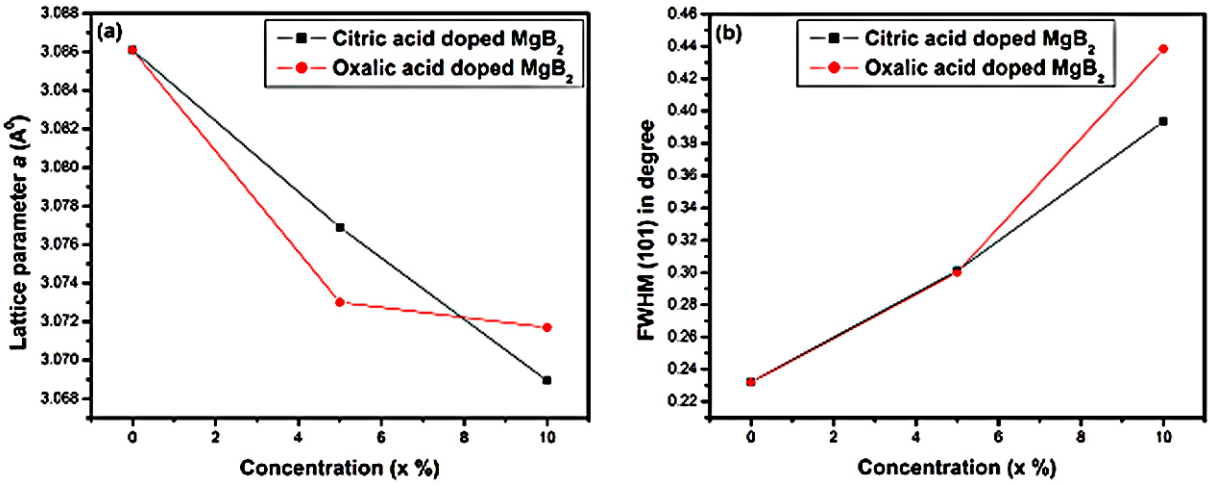

Figure 2. Variation of lattice parameter a (a) and FWHM (b) with doping concentration of citric and oxalic acids.

Table 1. Various parameters of undoped and doped MgB_2 samples.

Samples	T_C (K)	Lattice parameter (Å) a	c	FWHM (101)	$\rho_{300\ K}$ ($\mu\Omega$ cm)	$\rho_{40\ K}$ ($\mu\Omega$ cm)	A_F	Strain	Actual x in $Mg(B_{1-x}C_x)_2$	Crystallite size (μm)	Vol% of MgO
MgB_2	38.30	3.0861	3.5222	0.232	43.02	12.44	0.238	0.285		0.621	1.9
$MgB_2 + 5\%$ $C_6H_8O_7$	37.48	3.0769	3.5123	0.301	44.68	13.44	0.233	0.306	0.021	0.531	2.5
$MgB_2 + 10\%$ $C_6H_8O_7$	37.1	3.0689	3.5179	0.395	87.62	38.55	0.148	0.321	0.039	0.498	3.3
$MgB_2 + 5\%$ $C_2H_2O_4{\cdot}2H_2O$	36.73	3.076	3.5113	0.299	53.17	19.45	0.216	0.231	0.017	0.511	2.3
$MgB_2 + 10\%$ $C_2H_2O_4{\cdot}2H_2O$	36.4	3.0717	3.5112	0.438	64.83	26.45	0.190	0.556	0.032	0.478	3.2

value and crystallite size of the samples from the Williamson–Hall plot [24]. We find that the crystallite size decreases with doping concentration. The estimated values of microstrain are given in table 1. It can be seen that the value of microstrain increases (except for 5 wt% oxalic acid) with doping concentration of C in the samples. This suggests that inclusion of C increases distortion in the sample leading to a smaller crystallite size. The decreased crystallite size helps to enhance the flux pinning, since grain boundaries act as strong pinning centers [25, 26].

The microstructural characteristics of the samples have been studied by FESEM. Figure 3 shows FESEM micrographs of the undoped and 10 wt% citric and oxalic acid doped samples. The FESEM micrograph of the undoped sample (figure 3(a)) reveals the presence of isolated grains of various shapes, like circles, bars and cylinders. On the other hand, in the case of doped samples we see clustering of grains (see figure 3(b) and (c)). The average crystallite sizes of the doped samples are smaller than those of undoped ones. This result is in conformity with the XRD results.

Figure 4 shows the resistivity versus temperature plots of doped and undoped MgB_2 samples. The transition temperatures (T_C) determined from the plots are 38.3, 37.1 and 36.4 K, respectively, for undoped, 10 wt% citric acid ($C_6H_8O_7$) doped and 10 wt% oxalic acid ($C_2H_6O_5$) doped MgB_2 samples (see table 1). From the figure 4 it is clear that the resistivities of the doped samples increase with increasing doping concentration. This indicates increased impurity scattering in the doped samples as a result of C substitution for B or C diffusion in the MgB_2 lattice as interstitial atoms. In addition to this, increased MgO content in the doped samples may be responsible for enhancement in the normal state resistivity and reduction in T_C of the doped samples. Figure 5 shows the T_C versus actual C content plots for both citric acid doped and oxalic acid doped samples. From the plots we find that T_C is not monotonically decreasing with %C; this suggests that MgO and C at grain boundaries also have some role in the reduction of T_C [27, 28]. The effective cross-sectional area, used to estimate the impurity scattering, has been calculated by the equation $A_F = \Delta\rho_{ideal}/(\rho_{300\ K} - \rho_{40K})$, proposed by Rowell [29]. $\Delta\rho_{ideal}$ is the ideal change in resistivity from 300 to 40 K for a fully connected sample, and its value is taken to be 7.3 $\mu\Omega$ cm [30]. The calculated values of A_F are given in table 1. It can be seen that A_F values of the doped samples are smaller than those of undoped one. This indicates poor connection and high intragrain scattering in the doped samples [21]. The poor connectivity due to the presence of impurity phase MgO and extra C at the grain boundaries

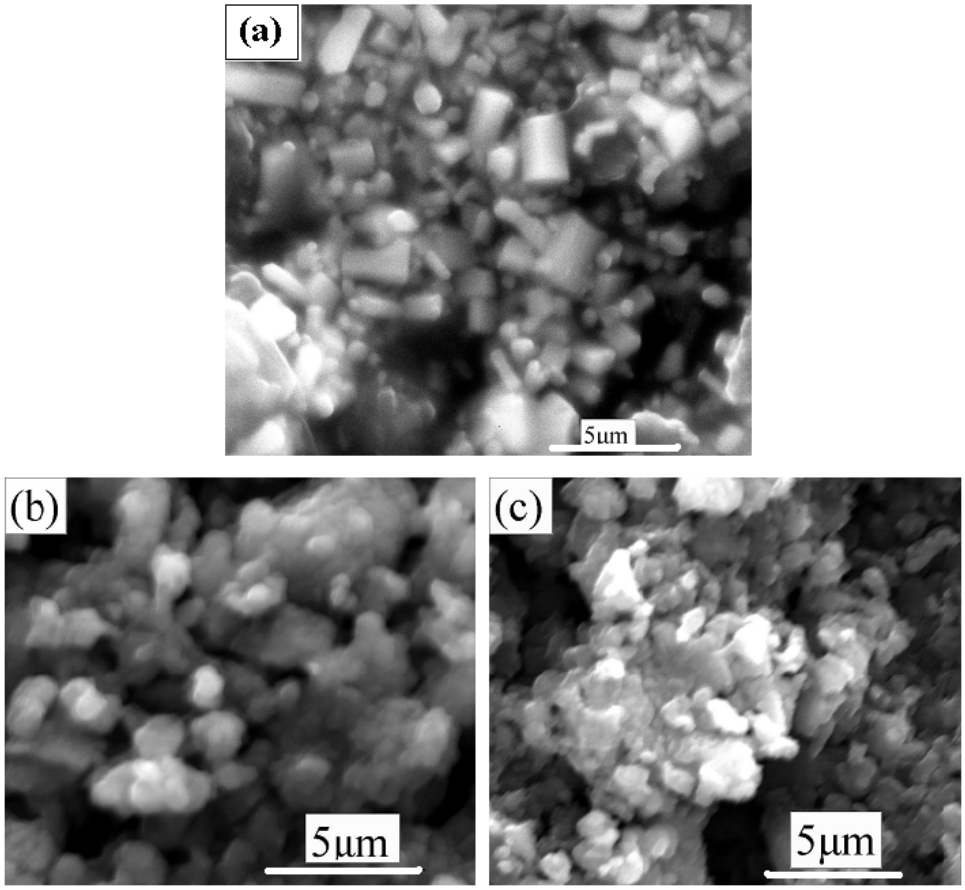

Figure 3. FESEM images of undoped (a), 10% citric acid doped (b) and 10% oxalic acid doped (c) MgB_2 samples.

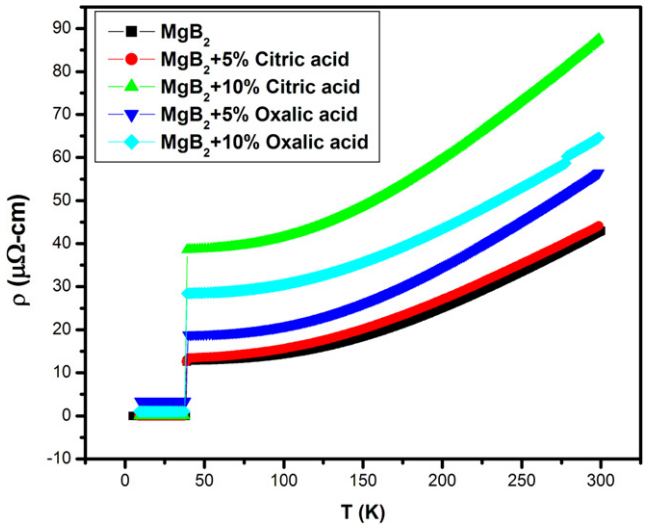

Figure 4. Resistivity versus temperature plots of undoped and doped MgB_2 samples.

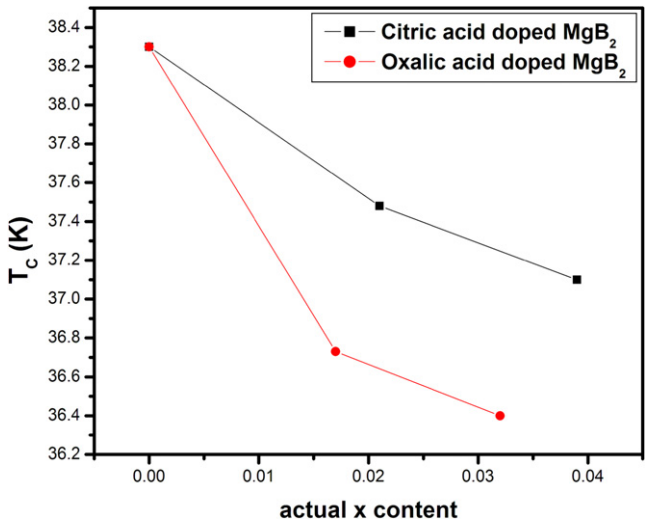

Figure 5. Variation of T_C with actual C content (x) in doped samples.

and high intragrain scattering is responsible for the higher resistivity of the doped samples compared to the undoped one. The variation of $\rho_{40\,K}$ with A_F is shown in figure 6. It can be seen that $\rho_{40\,K}$ decreases linearly with A_F. From table 1 we can also see that T_C decreases with increasing A_F. These results suggest that the connectivity and intragrain scattering are responsible for the variation of transition temperature with doping concentration of citric and oxalic acids.

$H_{C2}(T)$ and $H_{irr}(T)$ have been calculated from the field dependence R–T plots of figure 4 using the criteria 90% and 10% of normal state resistivity, respectively. The variations of $H_{C2}(T)$ and $H_{irr}(T)$ as a function of reduced temperature

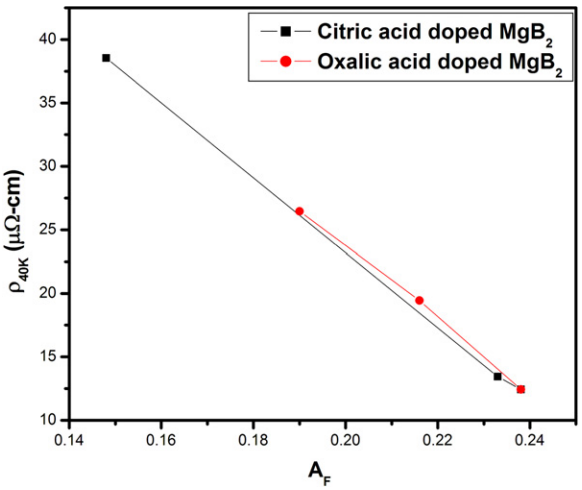

Figure 6. $\rho_{40\ \mathrm{K}}$ versus A_{F} for citric and oxalic acid doped MgB_2 samples.

(T/T_{C}) are shown in figures 7 and 8. Clearly, as a result of C doping, the H_{C2} and H_{irr} versus T/T_{C} curves become steeper, indicating improvement in H_{C2} and H_{irr} of the C doped samples as compared to the undoped one. We know that H_{C2} is related with coherence length according to the relation $H_{\mathrm{C2}} = \Phi_o/(2\pi\mu_o\xi^2)$, where ξ is the coherence length, Φ_o the superconducting flux quantum and μ_o the magnetic permeability [21]. This relation tells us that H_{C2} increases as ξ decreases. Since ξ increases with the mean free path, therefore, all the factors influencing the mean free path will change H_{C2}. In the doped samples the mean free path decreases due to lattice distortion and scattering from the substituting and interstitial C atoms, leading to enhancement in H_{C2}. From the XRD and FESEM results we have seen decrease in the crystallite size of the doped samples, i.e. increase in the number of grain boundaries. The impurity phases like MgO and unreacted carbon are also expected to distribute at the grain boundaries. Thus in the doped samples there are more flux pinning centers leading to improvement in their H_{irr} values. A comparison of the temperature dependence of H_{C2} and H_{irr} of 10 wt% citric and oxalic acid doped samples is shown in figure 9. From this figure it is clear that H_{C2} and H_{irr} values of citric acid doped sample are slightly higher than that of oxalic acid doped one at all temperatures. From the XRD results we have

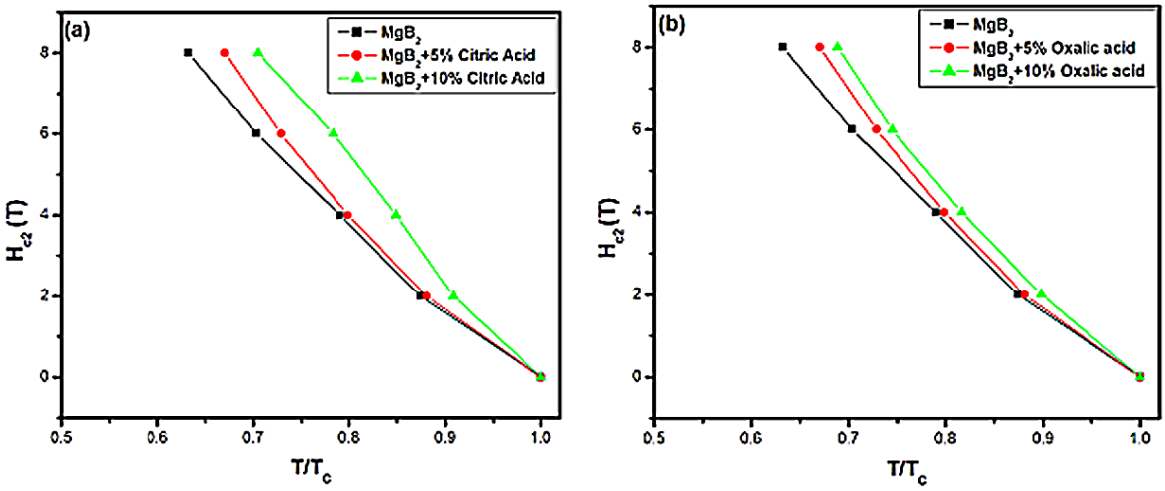

Figure 7. (a) Temperature dependence of H_{C2} (T) of the citric acid (a) and oxalic acid (b) doped MgB_2 samples.

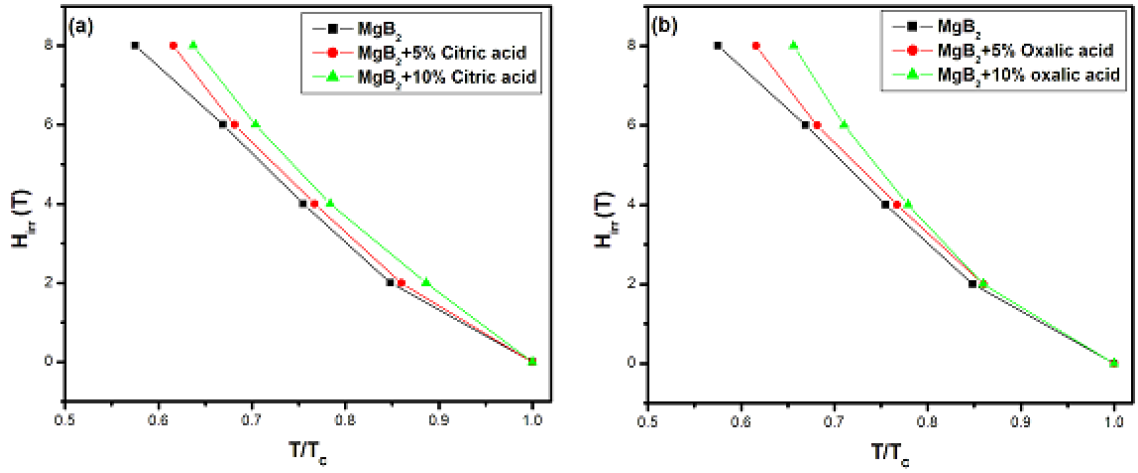

Figure 8. Temperature dependence of H_{irr} for the citric acid (a) and oxalic acid (b) doped MgB_2 samples.

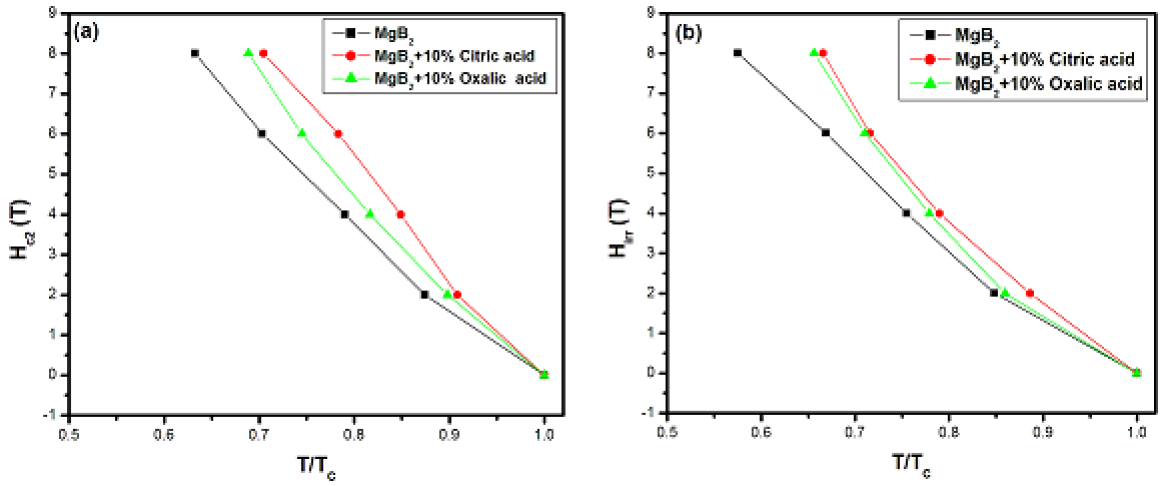

Figure 9. Temperature dependence of $H_{C2}(T)$ (a) and $H_{irr}(T)$ (b) of undoped, 10 wt% citric acid and 10 wt% oxalic acid doped MgB_2 samples.

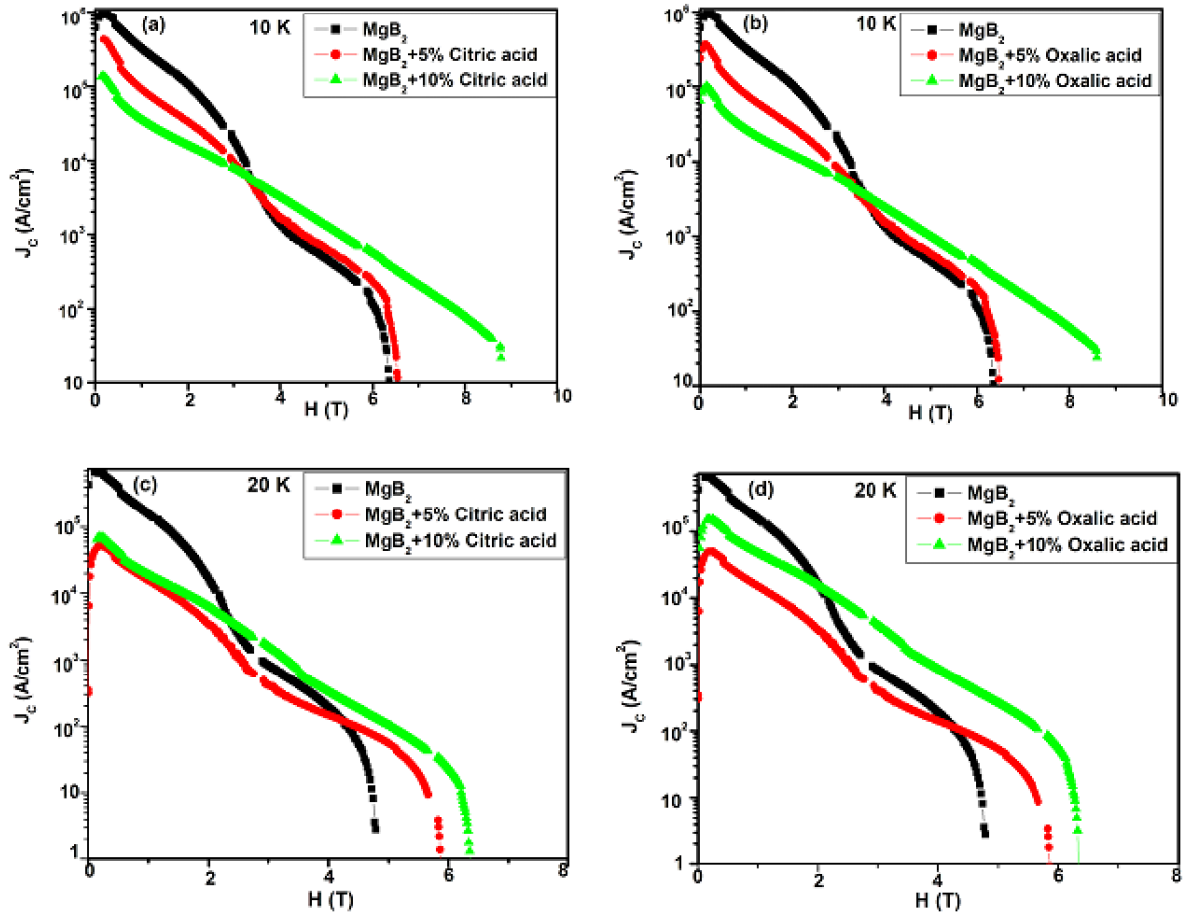

Figure 10. J_C (H) plots for citric acid doped ((a), (c)) and oxalic acid doped ((b), (d)) MgB_2 samples at 10 and 20 K.

seen more reduction in lattice parameter a with respect to the undoped sample for thr 10 wt% citric acid doped sample than the 10 wt% oxalic acid doped one. This suggests that there is more scattering from the doped C atoms in the citric acid doped sample compared to the oxalic acid doped one and therefore higher values of H_{C2} for earlier samples. The possible reason for the higher H_{irr} values of the citric acid doped sample compared to the oxalic acid doped one is a greater MgO content in the earlier sample as seen from the XRD results.

The critical current densities (J_C) of doped and undoped samples at 10 and 20 K were calculated from the M–H hysteresis loops by using Bean's critical state model [31]. The

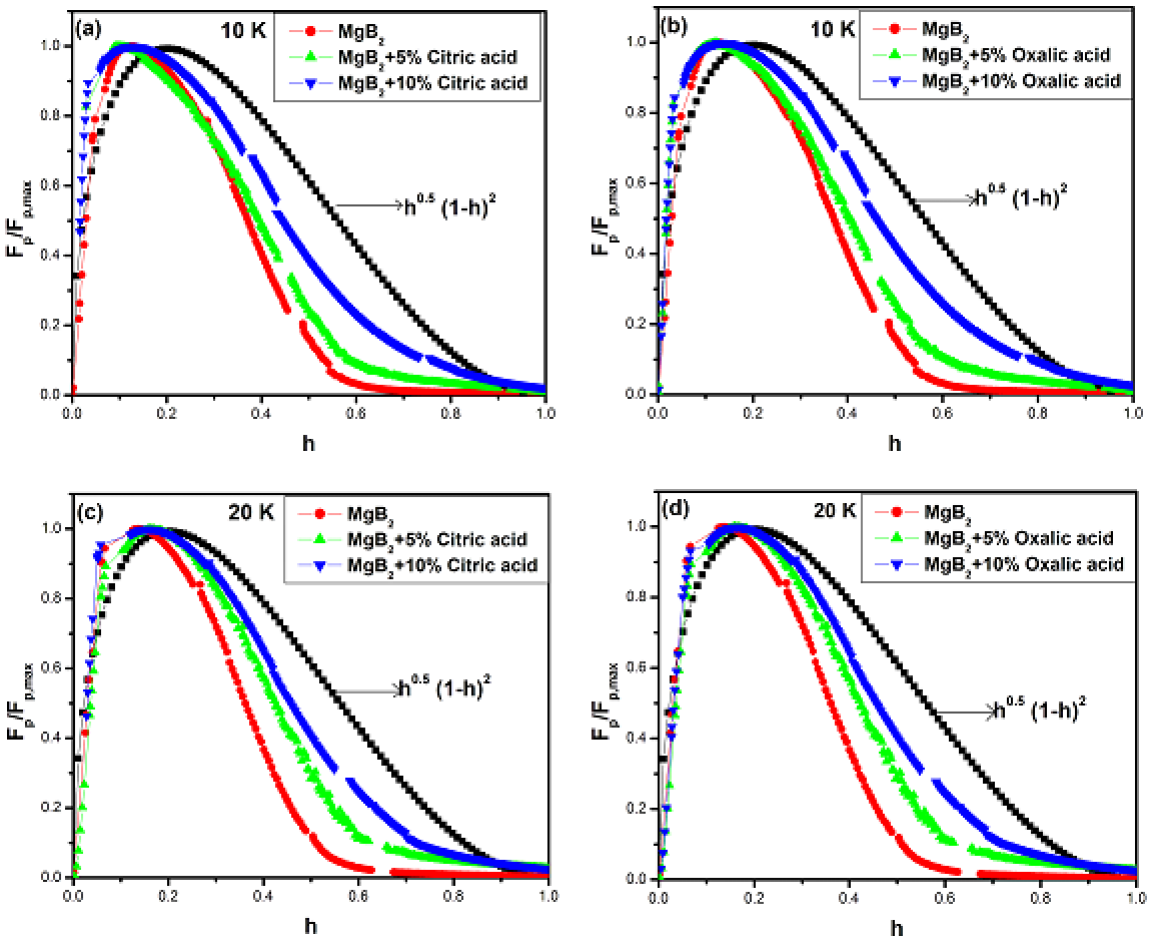

Figure 11. $F_p/F_{p,max}(F_p)$ versus H/H_{irr} (h) plots for citric acid doped ((a), (c)) and oxalic acid doped ((b), (d)) MgB_2 samples at 10 and 20 K.

average crystallite sizes used for calculation of the J_C values are given in table 1. Figure 10 shows the dependence of the critical current density (J_C) of the pure and doped samples on the applied magnetic fields at 10 and 20 K. From the 10 K plots we can see that self-field J_C decreases with the doping concentration of C in the samples. This is because of the greater lattice distortion and more impurity phases like MgO and unreacted C at the grain boundaries in the doped samples. However, we see improvement in J_C values of doped samples as compared to the undoped one in higher fields (>2.5 T) (see figure 10(a) and (b)). At 10 K and a 4 T field the J_C values of undoped and 10 wt% citric and oxalic acid doped samples are $\sim 1.35 \times 10^3$, 3.23×10^3 and 2.50×10^3 A cm^{-2}, respectively. At 20 K also the self-field J_C values of doped samples are lower than that of the undoped one. But here the self-field J_C value of 10 wt% doped samples is higher than that of 5 wt% doped samples. At 20 K we also see improvement in the J_C values of doped samples in higher fields with respect to undoped one (see figures 10(c) and (d)). The improvement in the J_C values of doped samples in the applied field is an indication of the increased pinning strength in the doped samples.

In order to study the nature of the pinning mechanisms we have calculated the volume pinning force, $F_p = J_C \times B(T)$, of undoped and doped samples at 10 and 20 K. The normalized volume pinning forces $F_p = F_p/F_{p,max}$ (where $F_{p,max}$ is the maximum pinning force) are plotted against the reduced magnetic field $h = H/H_{irr}$ in figures 11 at 10 and 20 K. Here the H_{irr} value has been taken as the field at which J_c becomes 100 A cm^{-2}. It has been observed that if pinning is arising due to the grain boundary, F_p follows a $h^{0.5}(1-h)^2$ dependence with a maximum value of F_p at $h = 0.2$ (see figure 11) [32, 33], and the F_p versus h curves overlap if a single pinning mechanism is involved. In our case F_p versus h curves do not overlap and maximum values of F_p occur at h varying in the range 0.12–0.17 (see figure 11); this suggests that there is more than one pinning mechanism involved in the samples. It can be seen from figure 11 that at both temperatures the values of F_p for h varying in the range 0.4–0.7 increase systematically with increasing doping levels. This may be explained in terms of two grain boundary pinning factors: grain size and dirtiness of the superconducting matrix. It has been pointed out that electron scattering pinning at the grain boundary (known as δk pinning) is strongly dependent upon the purity of the sample [34]. From the XRD results we have seen that crystallinity decreases and lattice distortion increases with increasing doping concentration in samples, which results in enhanced grain boundary flux pinning. Further, the nanosized impurity phases like MgO and unreacted C present in the doped samples act as point pinning centers, leading to improvement in their $J_C(H)$ values.

4. Summary

In summary, polycrystalline C doped MgB_2 samples have been prepared by using oxalic and citric acids as two carbon source materials. A systematic decrease in the lattice parameter a with increasing doping level confirms the substitution of C at the B site of MgB_2. It has been found that H_{C2} at a particular temperature ($<T_C$) systematically increases with increasing doping concentration. This is due to enhanced lattice distortion in the samples caused by C substitution for B and diffusion of C atoms in the MgB_2 lattice as interstitial atoms. Further, improvement in H_{irr} and high field (>2.5 T) J_C of the doped samples has been observed as compared to undoped one due to improved flux pinning in the doped samples. Based on the observed values of $J_C(H)$, H_{irr} and H_{C2} it can be concluded that the 10% citric acid doped sample is the best of the studied samples.

Acknowledgments

This work was supported by MHRD (Government of India), CSIR (Government of India). The authors are grateful to Dr Rajiv Rawat (UGC-DAE CSR, Indore) for doing R–T measurements in magnetic fields.

References

[1] Nagamatsu J, Nakagawa N, Muranaka T, Zenitanl Y and Akimitsu J 2001 *Nature* **410** 63
[2] Dou S X *et al* 2007 *Phys. Rev. Lett.* **98** 097002
[3] Dou S X, Soltanian S, Horvat J, Wang X L, Zhou S H, Ionescu M, Liu H K, Munroe P and Tomsic M 2002 *Appl. Phys. Lett.* **81** 3419
[4] Wilke R H T, Bud'ko S L, Canfield C, Finnemore D K, Suplinskas R J and Hannahs S T 2004 *Phys. Rev. Lett.* **92** 217003
[5] Kumakura H, Kitaguchi H, Matsumoto A and Hatakeyama H 2004 *Appl. Phys. Lett.* **84** 3669
[6] Kim J H, Yeoh W K, Qin M J, Xu X and Dou S X 2006 *J. Appl. Phys.* **100** 013908
[7] Sumption M D, Bhatia M, Rindfleisch M, Tomsic M, Soltanian S and Dou S X 2005 *Appl. Phys. Lett.* **86** 092507
[8] Bugoslavsky Y, Perkins G K, Qi X, Cohen L F and Caplin A D 2001 *Nature* **410** 561
[9] Fluiger R, Suo H L, Musolino N, Beneduce C, Toluemode P and Lezza P 2003 *Physica* C **385** 286
[10] Matsumoto A, Kumakura H, Kitaguchi H and Hatakeyama H 2003 *Supercond. Sci. Technol.* **16** 926
[11] Zhao Y, Feng Y, Huang D X, Machi T, Cheng C H, Nakao K, Chikumoto N, Fudamoto Y, Koshizuka N and Murakami M 2002 *Physica* C **378** 122
[12] Wang J, Bugoslavsky Y, Berenov A, Cowey L, Caplin A D, Cohen L F and MacManus Driscoll J L 2002 *Appl. Phys. Lett.* **81** 2026
[13] Yeoh W K, Kim J H, Horvat J, Dou S X and Munroe P 2006 *Supercond. Sci. Technol.* **19** L5
[14] Zeng R, Lu L and Dou S X 2008 *Supercond. Sci. Technol.* **21** 085003
[15] Serrano G, Serquis A, Dou S X, Soltanian S, Civale L, Maiorov B, Holesinger T G, Balakirev F and Jaime M 2008 *J. Appl. Phys.* **103** 023907
[16] Yeoh W K, Horvat J, Dou S X and Keast V 2004 *Supercond. Sci. Technol.* **17** S572
[17] Yamamoto A, Shimoyama J, Ueda S, Iwayama I, Horii S and Kishio K 2005 *Supercond. Sci. Technol.* **18** 1323
[18] Zhou S, Pan A V, Wexler D and Dou S X 2007 *Adv. Mater.* **19** 1373
[19] Yamada H, Hirakawa M, Kumakura H and Kitaguchi H 2006 *Supercond. Sci. Technol.* **19** 175
[20] Kim J H, Zhou S M, Hossain S A, Pan A V and Dou S X 2006 *Appl. Phys. Lett.* **89** 142505
[21] Zhang Y, Zhou S H, Lu C, Konstantinov K and Dou S X 2009 *Supercond. Sci. Technol.* **22** 015025
[22] Vajpayee A, Awana V P S, Bhalla A N, Bhope P A, Nigam A K and Kishan H 2009 *Supercond. Sci. Technol.* **22** 015016
[23] Lee S, Masui T, Yamamoto A, Uchiyama H and Tajima S 2003 *Physica* C **397** 7
[24] Williamson G K and Hall W H 1953 *Acta Metall.* **1** 22
[25] Martínez E, Mikheenko P, Martínez-López M, Millán A, Bevan A and Abell J S 2007 *Phys. Rev.* B **75** 134515
[26] Yamamoto A, Shimoyama J, Ueda S, Kastura Y, Iwayama I, Horii S and Kishio K 2005 *Appl. Phys. Lett.* **86** 212502
[27] Feng Y, Zhao Y, Pradhan A K, Cheng C H, Yau J K F, Zhou L, Koshizuka N and Murakami M 2002 *J. Appl. Phys.* **92** 2614
[28] Pogrebnyakov A V *et al* 2004 *Appl. Phys. Lett.* **85** 2017
[29] Rowell J M 2003 *Supercond. Sci. Technol.* **16** R17
[30] Canfield C, Finnemore D K, Bud'ko S L, Ostenson J E, Lapertot G, Cunningham C E and Petrovic C 2001 *Phys. Rev. Lett.* **86** 2423
[31] Beans C P 1964 *Rev. Mod. Phys.* **36** 31
[32] Dew-Huges D 1987 *Phil. Mag.* B **55** 459
[33] Tarantini C *et al* 2007 *Physica* C **463** 211
[34] Yetter W E, Thomas D A and Kramer E J 1982 *Phil. Mag.* B **46** 523